EDGE ARTICLE

Check for updates

Reactions of organic peroxy radicals, RO2, with substituted and biogenic alkenes at room temperature: unsuspected sinks for some RO2 in the atmosphere?†

Barbara Nozière [ID] ‡*[a] and Fabienne Fache [ID] [b]

Until now the reactions of organic peroxy radicals (RO2) with alkenes in the gas phase have been essentially studied at high temperature ($T \geq 360$ K) and in the context of combustion processes, while considered negligible in the Earth's atmosphere. In this work, the reactions of methyl-, 1-pentyl- and acetylperoxy radicals (CH3O2, C5H11O2, and CH3C(O)O2, respectively) with 2-methyl-2-butene, 2,3-dimethyl-2-butene and for the first time the atmospherically relevant isoprene, α-pinene, and limonene were studied at room temperature (298 ± 5 K). Monitoring directly the radicals with chemical ionization mass spectrometry led to rate coefficients larger than expected from previous combustion studies but following similar trends in terms of alkenes, with (in molecule^{-1} cm^3 s^{-1}) $k^{II}_{CH_3O_2} = 10^{-18}$ to $10^{-17} \times 2/2$ and $k^{II}_{CH_3CO(O)O_2} = 10^{-14}$ to $10^{-13} \times 5/5$. While these reactions would be negligible for CH3O2 and aliphatic RO2 at room temperature, this might not be the case for acyl-, and perhaps hydroxy-, allyl- and other substituted RO2. Combining our results with the Structure–Activity Relationship (SAR) predicts k^{II}(298 K) $\sim 10^{-14}$ molecule^{-1} cm^3 s^{-1} for hydroxy- and allyl-RO2 from isoprene oxidation, potentially accounting for up to 14% of their sinks in biogenic-rich regions of the atmosphere and much more in laboratory studies.
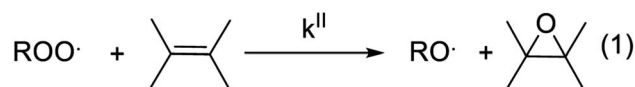
Introduction

Gas-phase organic peroxy radicals (RO2, where "R" is an organic moiety) play key roles in the chemistry and oxidizing capacity of the lower atmosphere. Atmospheric RO2 displays a wide variety of molecular structures, providing them with very different reactivities and rate coefficients often spanning over several orders of magnitude. Because of the difficulty in monitoring these radicals in the atmosphere, some unknowns remain in the details of their chemistry, which limit the understanding of atmospheric radical cycles. In particular, the measurements of OH and HO2 radical concentrations in the atmosphere have consistently reported discrepancies with models, especially in organic-rich and vegetation-impacted regions, which were attributed to unknown sinks for RO2.[1,2] Over the last decade, the identification of previously overlooked reactions of RO2 was able to reduce these discrepancies.[3,4] But recent studies have confirmed the persistence of differences, indicating the occurrence of unknown processes consuming RO2 and producing OH.[5,6]

RO2 can react with a wide range of chemical compounds, including unsaturated organic molecules, such as alkenes, forming the corresponding alkene epoxy as the main product (Scheme 1). Until now, these reactions have been essentially studied for their interest in combustion processes and, with a few exceptions, investigated experimentally at high temperature ($T \geq 360$ K).[7] Extrapolating these results suggest that these reactions are negligible at room temperature, and thus in the Earth's atmosphere. To our knowledge, they have never been considered in atmospheric chemistry.

Experimental values for the rate coefficients for these reactions, k^{II} (molecule^{-1} cm^3 s^{-1}), are scarce, in particular for CH3O2 (ref. 8) and CH3C(O)O2.[9] Ref. 7 summarizes these data and recommends expressions for $k^{II}(T)$, with $T = 360$–800 K,

[a]IRCELYON, CNRS and Université Claude Bernard Lyon 1, 2 Avenue Albert Einstein, 69626 Villeurbanne, France. E-mail: noziere@kth.se

[b]Université Lyon 1, CNRS, UMR 5246, Institut de Chimie et Biochimie Moléculaires et Supramoléculaires, 69626 Villeurbanne, France

† Electronic supplementary information (ESI) available. See DOI: 10.1039/d1sc02263f

‡ Now at KTH, Royal Institute of Technology, Teknikringen 30, 114 28 Stockholm, Sweden.

Scheme 1 General scheme for the reaction of RO2 with unsaturated compounds.

fitted to the experimental results. For most of the RO_2 listed, extrapolating these expressions to 298 K leads to $k^{II} \leq 10^{-19}$ molecule^{-1} cm^3 s^{-1}, thus justifying the omission of these reactions in atmospheric chemistry. But for some RO_2 such as $CH_3C(O)O_2$, the rate coefficients are 5 to 6 orders of magnitude larger than for CH_3O_2, suggesting that these reactions might not be entirely negligible at room temperature. Extrapolating the expressions in ref. 7 also results in uncertainties on the rate coefficients at 298 K of about ×10/10 for CH_3O_2 and ×30/30 for $CH_3C(O)O_2$, further justifying experimental studies. Finally, as previous studies focused exclusively on combustion systems, atmospherically relevant biogenic alkenes such as isoprene or terpenes have never been investigated. To our knowledge, the reaction of RO_2 with conjugated alkenes such as isoprene, prone to allylic rearrangement, has not been studied either. The reactions of RO_2 with biogenic alkenes at room temperature are thus worth investigating as a potential sink for at least some RO_2 in the atmosphere.

In this work, RO_2 + alkene reactions were investigated experimentally for the methyl peroxy radical, CH_3O_2, 1-pentyl peroxy radical, hereafter referred to as $C_5H_{11}O_2$, and peroxy acyl radical, $CH_3C(O)O_2$, with 2-methyl-2-butene, 2,3-dimethyl-butene, isoprene, α-pinene, and limonene at 298 ± 5 K.

Experimental section

Experimental conditions

The complete list of experiments is given in Section S1 of the ESI.† The experiments were performed in a vertical quartz

reactor of length L = 120 cm and internal diameter d = 5 cm, previously described in ref. 10 (Fig. 1) and operated in a continuous flow. The bath gas (synthetic air, 3–4 sLm, standard temperature = 273 K and pressure = 1 atm) and the radical precursors (CH_4, CH_3I, $C_5H_{11}I$, CH_3CHO and, where necessary, Cl_2) were introduced at the top of the reactor. Under these conditions, the gas flow was well in the laminar regime, with a Reynolds number of about 150. At the bottom of the reactor (z = 120 cm in Fig. 1), 1–4% of the flow mixture was sampled into a Chemical Ionization Mass Spectrometer (CIMS) using proton transfer as the ionization method.[11,12] The CIMS monitored continuously the RO_2 and stable compounds in the reactions at a residence time of 17 s and recorded their changes as alkenes were periodically added to the reactor (Fig. 2A), which were then used in the kinetic analysis.

The temperature and relative humidity inside the reactor were determined in separate sets of experiments, but under the same conditions of pressure, flow, and UV-light irradiation, by placing an infrared hygrometer (Extech 101) inside the reactor. The uncertainties of ±5 K attributed to the temperature include
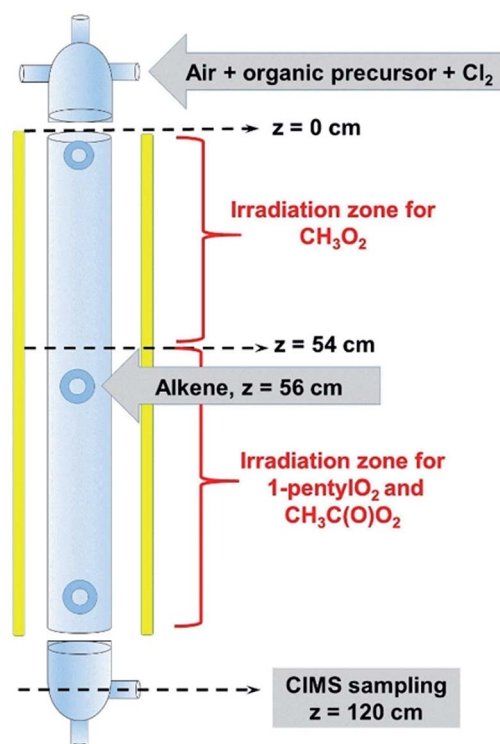

Fig. 1 Schematics of the reactor used for the experiments.
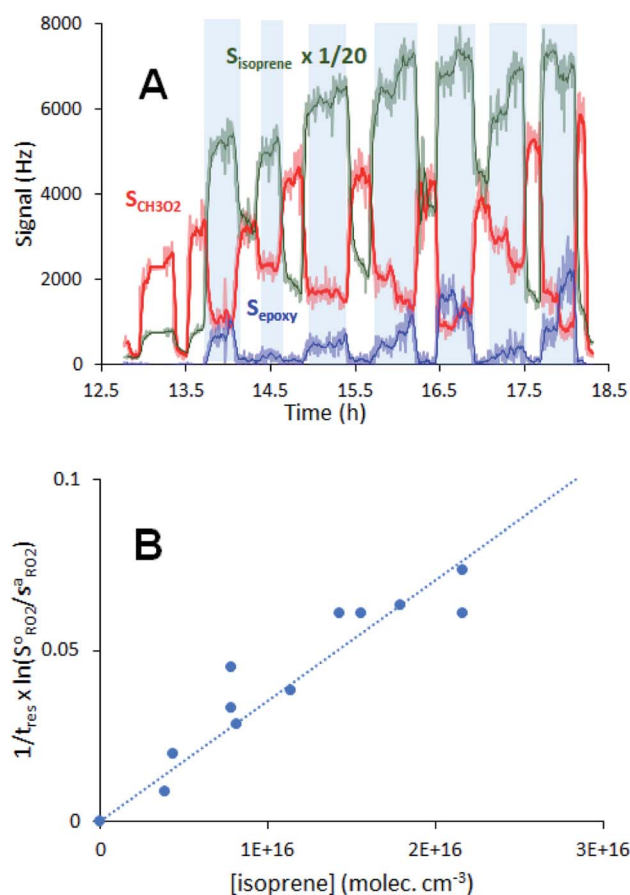
Fig. 2 Typical experimental profiles and kinetic analysis for the reaction CH_3O_2 + isoprene (experiment Alk03 in Table S1†): (A) real-time evolution of CH_3O_2 concentration (red line, m/z = 84), isoprene (green line, m/z = 69) and production of isoprene epoxy (blue line, m/z = 121). The areas shaded in blue correspond to the periodic addition of isoprene; (B) corresponding first-order variation of the ratio $S^o_{RO_2}/S_{RO_2}$ as a function of isoprene concentration providing k^{II}(298 K).

both the variabilities during the experiments and over the entire time span of the study.

The RO_2 were produced photochemically by irradiating the reactor over the wavelengths 280–400 nm with four fluorescent lights (Philips TL12, 40 W). For CH_3O_2 and $CH_3C(O)O_2$, the radical was produced by photolyzing chlorine, Cl_2, in the presence of an organic precursor (CH_4, and CH_3CHO, respectively) as in ref. 11. For CH_3O_2 the sequence was:

$$Cl_2 + h\nu \rightarrow 2Cl \qquad (2)$$

$$Cl + CH_4 \rightarrow CH_3 + HCl \qquad (3)$$

$$CH_3 + O_2 + M \rightarrow CH_3O_2 + M \qquad (4)$$

And for $CH_3C(O)O_2$:

$$Cl + CH_3CHO \rightarrow CH_3C(O) + HCl \qquad (5)$$

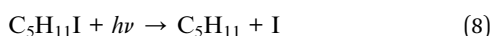$$CH_3C(O) + O_2 + M \rightarrow CH_3C(O)O_2 + M \qquad (6)$$
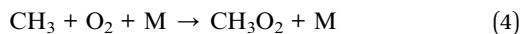
Irradiation tests were performed and confirmed that CH_3CHO was not photolyzed by the UV lights in the reactor and that its only fate was reaction.[5]

CH_3O_2 and $C_5H_{11}O_2$ were also produced by photolyzing directly their iodinated precursors, CH_3I and $C_5H_{11}I$, respectively, as in ref. 10. For CH_3O_2:

$$CH_3I + h\nu \rightarrow CH_3 + I \qquad (7)$$

Followed by reaction.[4] For $C_5H_{11}O_2$:

$$C_5H_{11}I + h\nu \rightarrow C_5H_{11} + I \qquad (8)$$

$$C_5H_{11} + O_2 + M \rightarrow C_5H_{11}O_2 + M \qquad (9)$$

CH_3O_2 was produced from two different precursors, CH_4 + Cl_2 and CH_3I, to rule out potential artefacts due to side-chemistry due to Cl_2/Cl or I atoms. Table S1† in the ESI provides the range of concentrations used for the different precursors. Only a small fraction of Cl_2 was photolyzed, leading to [Cl] in the range 10^{11} to 10^{12} molecule cm^{-3}.[12] In the systems using the photolysis of iodinated compounds, the number of radicals produced (thus of I atoms) was in the same range, based on the initial concentrations of RO_2 observed in this and previous studies.[10,11] In this study, the maximum RO_2 concentrations in the reactor were in the range 5×10^{10} to 5×10^{11} molecule cm^{-3} for CH_3O_2, $1–2 \times 10^{11}$ molecule cm^{-3} for $C_5H_{11}O_2$, and $1–3 \times 10^{10}$ molecule cm^{-3} for $CH_3C(O)O_2$.

Because the radicals studied had very different reactivities, different set-ups were used to study their reactions. CH_3O_2 was produced in the top half of the reactor ($z \leq 54$ cm in Fig. 1) and reacted with alkenes in the dark in the lower half ($z \geq 56$ cm), the alkenes being introduced at $z = 56$ cm (Fig. 1). This was not possible with $C_5H_{11}O_2$ and $CH_3C(O)O_2$, as producing them in the top half of the reactor resulted in non-measurable concentrations at the bottom ($z = 120$ cm). These radicals were thus produced in the bottom half of the reactor, the alkenes being still introduced at $z = 56$ cm. Thus, for these radicals,

photochemical production and reactions with alkenes occurred simultaneously in the lower half of the reactor. A separate series of experiments were performed and showed that the photolysis of RO_2 in the reactor was negligible, as was that of the stable reaction products (peroxides and aldehydes).

To avoid potential artefacts due to varying flow rate or pressure in the reactor when injecting the alkenes, the total flow through the alkene inlet was maintained continuous throughout the experiments using a flow controller toggled between pure N_2 and mixtures of alkenes in N_2. The existence of potential artefacts due to insufficient mixing of the alkenes in the reactor was also examined for CH_3O_2 by varying the total flow rate through the alkene inlet from 5 to 200 sccm, while maintaining the same alkene concentrations (using different dilution factors). The same results were obtained with all flow rates, indicating that such mixing effects were negligible under these conditions.

Chemicals

Gases. Synthetic air, 99.999%, CH_4, 1% in N_2, and Cl_2, 1% in N_2, all Air Products. A standard mixture of CH_3CHO 2950 ppm in N_2 was prepared by injecting 2 mL of the pure liquid in an evacuated 6 L cylinder and completing with high pressure N_2.

Liquids. CH_3CHO, $\geq$ 99.5%, Aldrich; CH_3I, 99% stabilized, Acros Organics; $C_5H_{11}I$, 97%, Acros; isoprene, 99%, Aldrich; α-pinene, 98%, Sigma; limonene, 97%, Aldrich; 2,3-dimethyl-2-butene, 98%, Acros. These liquids were placed in glass bubblers and introduced into the reactor by sending controlled flows of synthetic air or N_2 through the liquids. The gas-phase concentrations of these compounds in the reactor were then determined from the ratio of the alkene flow to the total flow and from the vapor pressure of the liquids at 298 K given in Table S2 of the ESI.†

Detection of RO_2, alkenes, and reaction products. The Chemical Ionization Mass Spectrometer (CIMS) used in this study employs proton transfer as the ionization method.[10–12] A compound A was thus detected by undergoing proton transfer with the parent ions H_3O^+ and its water clusters, $H_3O^+(H_2O)_n$ (with $n = 1–5$), following the reaction:

$$A + H_3O^+(H_2O)_n \rightarrow AH^+(H_2O)_m + (n - m + 1)H_2O \qquad (10)$$
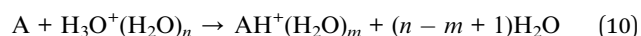
A compound of molecular mass M was thus detected by its ion products at $m/z = M + 1$, $M + 19$, $M + 37$, $M + 55$, $M + 73$, *etc.* Previous studies have shown that a CIMS instrument operating on this principle can detect volatile RO_2 in addition to stable molecules.[10–12] As in our previous studies,[10,11] the potential contribution of other compounds than RO_2 at their expected m/z was investigated by adding an excess of NO in the reactor, before or after the series of RO_2 + alkene experiments. These tests showed that less than 10% of the signals came from other compounds than RO_2, which was attributed to impurities in the system. These constant contributions to the RO_2 signals however cancelled out in the first-order kinetic analysis used in this work. In the presence of alkenes, the contribution of other compounds to the RO_2 m/z was not expected because the latter

have even values while stable $C_xH_yO_z$ compounds have odd m/z values with proton transfer.

The CIMS allowed monitoring continuously, with a time resolution of $\sim$1 s, the evolution of RO_2, alkenes, and stable reaction products as the alkenes were periodically added to the reactor (Fig. 2A). Table S3 of the ESI† gives the complete list of the ion masses at which these compounds were detected. Although knowing the absolute concentrations of RO_2 in the reactor was not necessary for the first-order kinetic analysis in this work (cf. "Kinetic analysis" below), they were determined in order to constrain the simulations that were used to validate these analyses (see "Kinetic simulations" below). For this, the detection sensitivities determined for these radicals in previous studies were used: $S^o_{(CH_3O_2)} = 5000$ Hz ppb^{-1},[10,11] $S^o_{(C_5H_{11}O_2)} = 200$ Hz ppb^{-1},[10] and $S^o_{(CH_3C(O)O_2)} = 2000$ Hz ppb^{-1}.[11]

For each reaction investigated, the occurrence of the reaction was confirmed by observing both the decrease of the RO_2 signal, S_{RO_2}, (thus of RO_2 concentration) upon alkene addition and by the build-up of stable products at the expected ion masses for the alkene epoxy (Fig. 2A).

Kinetic analysis

The rate coefficients, k^{II} (molecule^{-1} cm^3 s^{-1}), for the reactions RO_2 + alkene were determined experimentally from the ratios of the RO_2 signal between the absence and the presence of alkene, measured with the CIMS at the bottom of the reactor, and a simple first-order expression.

For radicals produced in the top half of the reactor and reacting in the dark in the bottom half (CH_3O_2 in this study), the maximum radical concentration, $[RO_2]_i$, is reached near mid-reactor ($z \sim 54$ cm in Fig. 1), and then decreases as a result of second-order sinks (self-reaction) and first-order sinks (wall losses, reactions with HO_2, potential isomerization... see Section S4 of the ESI† for the different RO_2) to reach $[RO_2]_o$ at $z = 120$ cm. Assuming that the second-order sinks are negligible, $[RO_2]_i$ and $[RO_2]_o$ are linked by a simple first-order expression:

$$\ln\left(\frac{[RO_2]_o}{[RO_2]_i}\right) = -k^I \times t_{res} \quad (11)$$

where k^I = sum of 1st order sinks and t_{res} = residence time between $z = 56$ and 120 cm ($\sim$17 s in this study). In the presence of alkenes, the reaction RO_2 + alkene adds another first-order term, further reducing $[RO_2]_o$ to $[RO_2]_a$ at $z = 120$ cm:

$$\ln\left(\frac{[RO_2]_a}{[RO_2]_i}\right) = -\left(k^I + k^I_{alkene}\right) \times t_{res} \quad (12)$$

with $k^I_{alkene} = k^{II} \times [alkene]$. Subtracting eqn (11) from eqn (12) thus gives:

$$\ln\left(\frac{[RO_2]_a}{[RO_2]_o}\right) = \ln\left(\frac{[SRO_2]_a}{[SRO_2]_o}\right) = -k^{II}_{alkene} \times [alkene] \times t_{res} \quad (13a)$$

thus:

$$k^{II}_{alkene} = -\frac{1}{[alkene]} \times \frac{1}{t_{res}} \times \ln\left(\frac{[SRO_2]_a}{[SRO_2]_o}\right) \quad (13b)$$

The rate coefficient k^{II} was then determined by applying eqn (13b) to the RO_2 signals measured in the absence and in the presence of alkenes with the CIMS. Eqn (13b) is, however, only an approximation of the kinetics for CH_3O_2 because of the potential contributions of second-order sinks, and even more so for $C_5H_{11}O_2$ and $CH_3C(O)O_2$ as these radicals were simultaneously produced and consumed in the reactor (Fig. 3 bottom). In addition, for all the radicals, the first-order sinks were not necessarily identical in the absence and in the presence of alkenes, as the concentrations of HO_2 (and of CH_3O_2 in the $CH_3C(O)O_2$ system) varied. Thus, kinetic simulations were run (next section) to determine the correction factors to apply to eqn (13b) to determine k^{II} in each series of experiments.

The correction factors for the reactions of CH_3O_2 were small (see below), implying only small uncertainties in the kinetic results, but larger for $C_5H_{11}O_2$ and $CH_3C(O)O_2$, implying larger uncertainties. The uncertainties in the values of k^{II} obtained from these analyses were thus estimated to be $\times 2/2$, for CH_3O_2, mostly based on the statistical dispersion, and $\times 5/5$ for the reactions of $C_5H_{11}O_2$ and $CH_3C(O)O_2$ because of the larger uncertainties in the correction factors and of the limited range of alkene concentrations that could be used in these experiments.
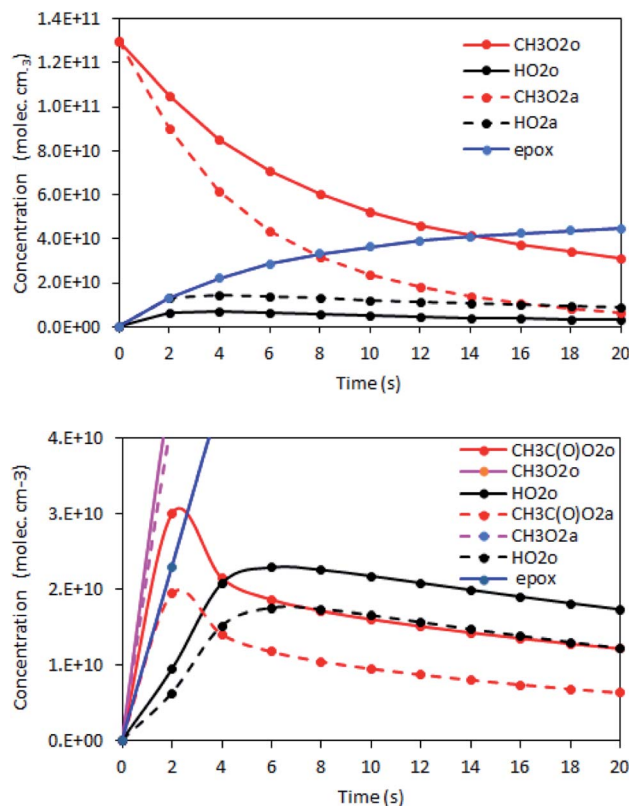

Fig. 3 Examples of simulations of the RO_2 + alkene reactions, showing the concentration profiles in the reactor for RO_2 (red and pink), HO_2 (black), and epoxy products (blue). The solid lines are the profiles in the absence of alkenes and the dashed ones in the presence of alkenes. Top: CH_3O_2 + isoprene reaction (experiment Alk05); bottom: $CH_3C(O)O_2$ + isoprene reaction (experiment Alk31).

Kinetic simulations

Kinetic simulations using Chemsimul (V3.90, 2018) were performed to validate our kinetic analysis and to quantify the correction factors to apply to eqn (13b) to determine k^{II} from the experimental data. Complete details on these simulations, including the chemical equations, rate coefficients, and numerical results, are given in Section S4 of the ESI.† Briefly, they consisted of calculating first the concentration profiles in the reactor with [alkene] = 0 and constraining $[RO_2]_o$ with the experimental RO_2 signals. Then, they were run again using alkene concentrations typical of the experiments to determine $[RO_2]_a$ (Fig. 3). Eqn (13b) was then applied to determine k^{II}. Comparing the k^{II} thus obtained at $t = 17$ s to the value assumed for this coefficient in the kinetic model gave the correction factor to apply to eqn (13b) in the kinetic analyses.

The results showed that, for CH_3O_2 reactions, the correction factor was 0.76, mostly compensating for neglecting the self-reaction and for the differences in the first-order sinks in the absence and presence of alkenes. For the reactions of $C_5H_{11}O_2$ and $CH_3C(O)O_2$, these factors were larger, ~5 and ~19, respectively, compensating for a number of contributions detailed in Section S4 of the ESI.†

Results and discussion

The rate coefficients, $k^{\mathrm{II}}(298\ \mathrm{K})$, obtained in this work are summarized in Fig. 4 and listed in Table S5† of the ESI. For the alkenes studied in this work they varied between about 2 and 7 $\times 10^{-18}$ molecule^{-1} cm^3 s^{-1} for CH_3O_2, 8 to 160 $\times 10^{-18}$ molecule^{-1} cm^3 s^{-1} for $C_5H_{11}O_2$ and 2 to 12 $\times 10^{-14}$ molecule^{-1} cm^3 s^{-1} for $CH_3C(O)O_2$. For all radicals, the rate coefficients followed similar trends in terms of alkene structure, the smallest coefficients being for isoprene and the largest for 2,3-dimethyl-2-butene. These results show that these reactions would be slow at room temperature for CH_3O_2, $C_5H_{11}O_2$, and probably other aliphatic RO_2 but not necessarily for $CH_3C(O)O_2$. These results also implied that, at room temperature, CH_3O_2 reacts about 18 times faster than HO_2, based on the rate coefficients for HO_2 + alkenes in ref. 7.

Comparison with high-temperature data and the Structure–Activity Relationship (SAR)

In Fig. 4, the rate coefficients obtained in this work are compared with those extrapolated from previous high-temperature studies (for those available).[7–9] The rate coefficients were also calculated for CH_3O_2, $CH_3C(O)O_2$ and the alkenes studied in this work using the Structure–Activity Relationship (SAR) recommended in ref. 7. For $C_5H_{11}O_2$, this could not be done because the required parameters were not available in the literature. For CH_3O_2 and $CH_3C(O)O_2$, the activation energy of each reaction, E (kJ mol^{-1}), was calculated from the charge-transfer energy, ΔEc (kJ mol^{-1}), using an equation recommended in ref. 7.
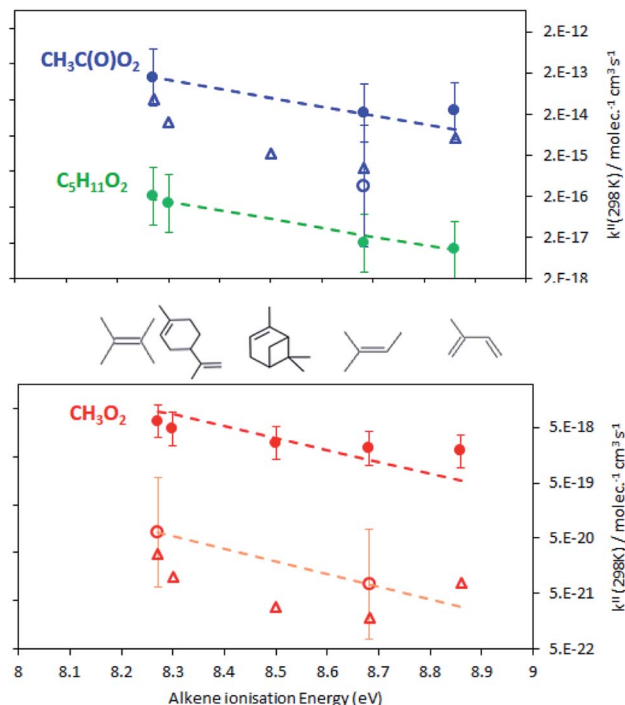
$$E = 83.0 - 1.82 \times \Delta Ec \qquad (14)$$

Fig. 4 Rate coefficients, $k^{\mathrm{II}}(298\ \mathrm{K})$, measured in this work (full circles) for the reactions of CH_3O_2 (red), $C_5H_{11}O_2$ (green), and $CH_3CO(O)O_2$ (blue) with various alkenes and comparisons with those extrapolated from high-temperature data (open circles) and predicted using the SAR (open triangles). Note that the results for α-pinene have been assigned an arbitrary ionisation energy of 8.5 eV in the graph and in the SAR. The dashed lines are linear regressions (excluding the data for isoprene, see the text).

ΔEc was itself determined from the absolute electronegativity, χ, and absolute hardness, η, of the radical and alkene involved, each determined from their ionization energy, I, and electron affinity A:

$$\Delta Ec = -(\chi_{RO_2} - \chi_{\mathrm{alkene}})^2/4 \times (\eta_{RO_2} - \eta_{\mathrm{alkene}}) \qquad (15)$$

with

$$\chi = (I + A)/2 \qquad (16)$$

$$\eta = (I - A)/2 \qquad (17)$$

The pre-exponential factor for the rate coefficients, A_o, used in these SAR calculations was the one recommended in ref. 7 and obtained from empirically fitting the combustion data: $A_o = 2.09 \times 10^{-13}$ molecule^{-1} cm^3 s^{-1}. The ionization energies, I, and electron affinities, A, used in these calculations and the values predicted for $k^{\mathrm{II}}(298\ \mathrm{K})$ are presented in Table 1.

Fig. 4 clearly shows that the $k^{\mathrm{II}}(298\ \mathrm{K})$ obtained in this work is larger than expected from the combustion data, by about a factor 60 for $CH_3C(O)O_2$ and 100 to 300 for CH_3O_2, and by factors 20 and 250 to 1000, respectively, from the SAR predictions. In addition, while the present results indicate that CH_3O_2 reacts 18 times faster than HO_2 (with 2,3-dimethyl-2-butene) the

Table 1 Parameters and SAR predictions for k^{II}(298 K) for various RO_2 and alkenes

	I (eV)	A (eV)	χ (eV)	η (eV)	ΔEc (kJ mol^{-1})	E (kJ mol^{-1})	k^{II} (298 K) molecule^{-1} cm^3 s^{-1}
2,3-Dimethyl-2-butene	8.27[a]	−2.27[b]	3.0	5.3			
Limonene	8.30[c]	−2.10[d]	3.1	5.2			
α-pinene	8.07[c]	−2.10[d]	3.2	5.3			
2-Methyl-2-butene	8.68[a]	−2.24[b]	3.2	5.5			
Isoprene	8.86[c]	−2.80[e]	3.0	5.8			
$CH_3C(O)O_2$	11.58[f]	2.75[f]	7.2	4.4			
CH_3O_2	11.18[f]	1.21[f]	6.2	5.0			
i-$C_3H_7O_2$ (H_3C–CHO_2–CH_3)	11.00[g]	1.40[g]	6.2	4.8			
$HOC_3H_6O_2$ ($HOCH_2$–CHO_2–CH_3)	11.86[g]	2.02[g]	6.4	4.4			
$C_3H_5O_2$ (H_2C=CH–CH_2O_2)	11.14[g]	1.60[g]	6.4	4.8			
$CH_3C(O)O_2$ + 2,3-dimethyl-2-butene					43.2	4.39	3.6×10^{-14}
$CH_3C(O)O_2$ + limonene					41.5	7.55	9.9×10^{-15}
$CH_3C(O)O_2$ + α-pinene					39.0	11.95	1.7×10^{-15}
$CH_3C(O)O_2$ + 2-methyl-2-butene					38.0	13.85	7.8×10^{-16}
$CH_3C(O)O_2$ + isoprene					40.3	9.73	4.1×10^{-15}
CH_3O_2 + 2,3-dimethyl-2-butene					24.0	39.31	2.7×10^{-20}
CH_3O_2 + limonene					22.7	41.71	1.0×10^{-20}
CH_3O_2 + α-pinene					21.0	44.71	3.0×10^{-21}
CH_3O_2 + 2-methyl-2-butene					20.4	45.83	1.9×10^{-21}
CH_3O_2 + isoprene					22.3	42.34	7.9×10^{-21}
i-$C_3H_7O_2$ + 2,3-dimethyl-2-butene					24.5	38.37	3.9×10^{-20}
$HOC_3H_6O_2$ + 2,3-dimethyl-2-butene					29.4	29.40	1.5×10^{-18}
$C_3H_5O_2$ + 2,3-dimethyl-2-butene					27.3	33.36	3.0×10^{-19}

[a] Ref. 14. [b] Ref. 15. [c] Ref. 13. [d] Based on cyclohexene in ref. 15 but corrected by −0.03 eV for each methyl group. [e] From ref. 15 but for two double bonds. [f] Ref. 16. [g] Ref. 7.

high-temperature data predicted it to react 6 times slower than HO_2.

Besides these discrepancies, the rate coefficients obtained in this work followed similar trends to the high-temperature experimental data and SAR previsions in terms of alkene substitution and RO_2 structure. In particular, for all the RO_2, k^{II}(298 K) increased with alkene substitution, including for the alkenes studied here for the first time, in the sequence isoprene < 2-methyl-2-butene < α-pinene < limonene < 2,3-dimethyl-2-butene. As explained in ref. 7 for an electrophilic addition of a RO_2 radical onto a double bond the activation energy, E, is expected to vary proportionally with the alkene ionization energy, which is implicit in eqn (14)–(17). In this work, k^{II} was indeed found to increase with alkene ionization energies (Table 1): isoprene, 8.86;[13] 2-methyl-2-butene, 8.68;[7] limonene, 8.30;[13] 2,3-dimethyl-2-butene, 8.27.[7] Only for α-pinene the ionization energy of 8.07 eV[13] found in the literature did not seem consistent with that of the similar molecule limonene. α-pinene was thus arbitrarily assigned an ionization energy of 8.5 eV in Fig. 4 and in the SAR calculations. With this, linear regressions (on the ln scale) were performed on the results, but excluding the data for isoprene (see discussion below).

These linear regressions (dashed lines in Fig. 4) allowed the estimation of k^{II}(298 K) for reactions that had not been studied. For instance, k^{II}(298 K) for $CH_3C(O)O_2$ + terpenes was estimated to be in the range 0.5–1 × 10^{-13} molecule^{-1} cm^3 s^{-1} (blue line in Fig. 4).

Leaving out the RO_2 + isoprene data from the linear regressions revealed that the k^{II}(298 K) for these reactions was systematically larger than the regressions (Fig. 4). These deviations corresponded to a factor 2.8 in average, thus providing an estimate for the excess reactivity due to allylic rearrangement in the RO_2 + isoprene reactions.

As explained in ref. 7 and implicit in the SAR calculations, k^{II} for RO_2 + alkene also varies strongly with the RO_2 structure. In the present work, for the same alkene, $CH_3C(O)O_2$ reacts 9000 to 18 000 times faster than CH_3O_2, while the combustion data predicted a ratio of 36 000 between these radicals with 2-methyl-2-butene. The SAR predicted even larger ratios, between 400 000 and 1 000 000, but the large discrepancies with the experimental data are likely due to the empirical determination of the preexponential factors.

The rate coefficients measured for $C_5H_{11}O_2$ in this work indicate that this radical reacts about 14 times faster than CH_3O_2 in average. This seems reasonable as the rate coefficients for other radicals (for instance i-$C_3H_7O_2$ in Table 1) indicate that k^{II} increases only by a small factor for each additional carbon atom. However, as no other experimental data were available for this radical and its ionization energy and electron affinity were not available, no further comparison could be made with these rate coefficients.

The large discrepancies between the rate coefficients obtained in this work and those reported at high temperature[7–9] seem difficult to reconcile, suggesting experimental or analytical artefacts in at least one of the data sets. In the present work,

monitoring directly RO_2 with only minor potential interference from other compounds should be more selective than monitoring the overall epoxide formation in previous studies.[8,9] And using a relative kinetic approach ("alkene off"/"alkene on") should limit the artefacts in the results by cancelling out a large part of the RO_2 sinks other than alkenes. The potential role of side-reactions involving OH radicals or Cl atoms was also investigated and ruled out by performing kinetic simulations (Section S4 of the ESI†). This was further confirmed by the fact that large discrepancies with the high-temperature results were obtained in this work with all types of precursors (Cl_2, iodinated compounds) and set-ups. One potential artefact that could account for the large rate coefficients in this work would be insufficient mixing, leading to large underestimations of the alkene concentrations. But, besides the fact that such mixing effects were ruled out by varying the total alkene flow rate (Experimental section), they should affect equally all the rate coefficients, while the discrepancies with the high-temperature data are much larger for CH_3O_2 than for $CH_3C(O)O_2$ reactions (by almost a factor of 5). As a further confirmation, the kinetic simulations showed that such large alkene concentrations would entirely consume RO_2, making it impossible to observe profiles such as that in Fig. 2B. While no obvious artefact accounting for the large discrepancies with the high-temperature data can be found in our work, identifying such an artefact in these previous studies[8,9] is not easy, especially as little information was provided on their kinetic analysis. In these previous studies, the rate coefficients were determined from the overall formation of the epoxy product. Thus, underestimating the contribution of HO_2 to this formation or overestimating the RO_2 concentrations, for instance by overlooking side-reactions, could have potentially underestimated the RO_2 + alkene rate coefficients.

Other RO_2 and alkenes leading to significant reactions at room temperature

Beyond $CH_3C(O)O_2$ and the substituted alkenes studied in this work, it would be interesting to identify other alkenes and RO_2 leading to significant reaction rates at room temperature. First, previous studies have shown that oxygenated substituents such as carbonyl groups further enhance the reactivity of unsaturated compounds compared to their alkene analogues. In particular the rate coefficient for the reaction of $CH_3C(O)O_2$ with C_2H_3CHO (acrolein)[17] was reported to be about 3 times the one with propene. This suggests that oxidation products from isoprene, such as methacrolein and methyl vinyl ketone, or from terpenes, or even unsaturated alcohols such as the biogenic compound 2-methyl-3-butene-ol, might react faster with RO_2 than isoprene or terpenes themselves.

The SAR, ionization energies and electron affinities in ref. 7 were also used to estimate the rate coefficients with 2,3-dimethyl-2-butene at 298 K for other RO_2 than those studied experimentally: isopropylperoxy, i-$C_3H_7O_2$ or $H_3C–CH_2O_2–CH_3$, 1-hydroxy-2-propylperoxy, $HOC_3H_6O_2$ or $HOCH_2–CHO_2–CH_3$, and allylperoxy, $C_3H_5O_2$ or $H_2C=CH_2–CH_2O_2$. The ionization energies, electron affinities, and results for these radicals are presented in Table 1. They show that, at 298 K, $HOC_3H_6O_2$ reacts about 40 times faster than its aliphatic analogue i-$C_3H_6O_2$. Allylperoxy, $C_3H_5O_2$, was predicted to react about 8 times faster than i-$C_3H_6O_2$, which was assumed to be a typical factor for allyl-substituents, in the absence of ionization energies and electron affinities allowing a comparison with the primary aliphatic analogue 1-$C_3H_6O_2$. Some RO_2 produced by the OH oxidation of isoprene contains both HO- and allyl-substituents, and thus their rate coefficients with alkenes might combine the above factors and be significant at room temperature. The rate coefficient with 2,3-dimethyl-2-butene for such C5-RO_2 can be roughly estimated from that of 1-$C_5H_{11}O_2$ measured in this work, $k^{II} \sim 1.5 \times 10^{-16}$ molecule^{-1} cm^3 s^{-1}, and the factors $\times 40$ and $\times 8$ for the HO- and allyl substituents, leading to 5×10^{-14} molecule^{-1} cm^3 s^{-1}. This estimate has for only purpose to make a first assessment of the importance of these reactions in the laboratory and in the atmosphere, and would obviously need to be confirmed by experimental studies.

Conclusions and atmospheric implications

The rate coefficients for RO_2 + alkene reactions at room temperature measured in this work were larger than expected from previous combustion studies. While those for many RO_2, in particular aliphatic ones, would still be small ($\leq 10^{-15}$ molecule^{-1} cm^3 s^{-1}), those for acyl-substituted RO_2 could be as large as 10^{-14} to 10^{-13} molecule^{-1} cm^3 s^{-1}. SAR predictions indicate that other substituents, such as HO- or allyl-, would also contribute to enhance the reactivity of RO_2 towards alkenes, especially when combined as for the RO_2 produced by the OH-oxidation of multi-unsaturated alkenes (isoprene, terpenes, …).

While these estimates await confirmation from further experimental studies, the importance of these reactions in the atmosphere and laboratory for the RO_2 produced by the OH-oxidation of isoprene can be determined from the rate coefficient estimated above. Assuming k^{II} (RO_2 + isoprene) $\sim 1/5 \times k^{II}$ (RO_2 + 2,3-dimethyl-2-butene) $= 10^{-14}$ molecule^{-1} cm^3 s^{-1} and typical isoprene concentrations of 10^{12} molecule cm^{-3} in the laboratory or smog chamber would correspond to RO_2 sinks of 0.01 s^{-1}. Note that, while some of these RO_2 radicals would rapidly undergo H-migration reactions,[3,18] their $HOOQO_2$ isomers would also carry HO- and allyl-groups, and thus have similar rate coefficients to alkenes. In the absence of NO, the main other sink for the RO_2 would be their reactions with HO_2. Typical HO_2 concentrations of 10^9 molecule cm^{-3} and a rate coefficient of 10^{-11} molecule^{-1} cm^3 s^{-1} also correspond to a sink of 0.01 s^{-1}, implying that the reactions with isoprene could represent as much as half of the RO_2 sinks under such conditions. If so, they should lead to measurable concentrations of isoprene epoxy, which might have been overlooked or mis-attributed in previous isoprene oxidation studies.[19] In the atmosphere, the concentrations reported (for instance in ref. 1) in vegetation-impacted regions, isoprene $= 5 \times 10^{10}$; NO $= 5 \times 10^8$; $HO_2 = 10^8$ molecule cm^{-3}, correspond to sinks for

isoprene-RO_2 (and $HOOQO_2$) of 0.0005, 0.002, and 0.001 s^{-1}, respectively. Reactions with isoprene could thus represent as much as 14% of the sinks for these RO_2 radicals, to which their reactions with methacrolein and methyl vinyl ketone would probably have to be added. Thus, for some RO_2, RO_2 + alkene reactions might not be negligible even in the atmosphere, which emphasizes the need for further experimental investigations at room temperature.

Data availability

Most of the data is presented in the ESI.†

Author contributions

BN: conceptualization; methodology; investigation; visualization; writing – original draft; FF: conceptualization; visualization; writing – original draft.

Conflicts of interest

The authors have no conflicts to declare.

Acknowledgements

References

1 J. Lelieveld, T. M. Butler, J. N. Crowley, T. J. Dillon, H. Fischer, L. Ganzeveld, H. Harder, M. G. Lawrence, M. Martinez, D. Taraborrelli and J. Williams, *Nature*, 2008, **452**, 737–740.

2 A. Hofzumahaus, F. Rohrer, K. Lu, B. Bohn, T. Brauers, C.-C. Chang, H. Fuchs, F. Holland, K. Kita, Y. Kondo, X. Li, S. Lou, M. Shao, L. Zeng, A. Wahner and Y. Zhang, *Science*, 2009, **324**, 1702–1704.

3 J. Peeters, T. L. Nguyen and L. Vereecken, *Phys. Chem. Chem. Phys.*, 2009, **11**, 5935–5939.

4 J. J. Orlando and G. S. Tyndall, *Chem. Soc. Rev.*, 2012, **41**, 6294–6317.

5 K. D. Lu, F. Rohrer, F. Holland, H. Fuchs, B. Bohn, T. Brauers, C. C. Chang, R. Häseler, M. Hu, K. Kita, Y. Kondo, X. Li, S. R. Lou, S. Nehr, M. Shao, L. M. Zeng, A. Wahner, Y. H. Zhang and A. Hofzumahaus, *Atmos. Chem. Phys.*, 2012, **12**, 1541–1569.

6 Z. Tan, K. Lu, A. Hofzumahaus, H. Fuchs, B. Bohn, F. Holland, Y. Liu, F. Rohrer, M. Shao, K. Sun, Y. Wu, L. Zeng, Y. Zhang, Q. Zou, A. Kiendler-Scharr, A. Wahner and Y. Zhang, *Atmos. Chem. Phys.*, 2019, **19**, 7129–7150.

7 M. S. Stark, *J. Phys. Chem. A*, 1997, **101**, 8296–8301.

8 D. A. Osbourne and D. J. Waddington, *J. Chem. Soc., Perkin Trans. 2*, 1980, 925–930.

9 R. Ruiz Diaz, K. Selby and D. J. Waddington, *J. Chem. Soc., Perkin Trans. 2*, 1977, 360–363.

10 B. Nozière and L. Vereecken, *Angew. Chem. Int. Ed.*, 2019, **58**, 13976–13982.

11 B. Nozière and D. R. Hanson, *J. Phys. Chem. A*, 2017, **121**, 8453–8464.

12 D. Hanson, J. Orlando, B. Nozière and E. Kosciuch, *Int. J. Mass Spectrom.*, 2004, **239**, 147–159.

13 J. E. Bartmess, NIST Chemistry WebBook, NIST Standard Reference Database Number 69, ed. P. J. Linstrom and W. G. Mallard, in *National Institute of Standards and Technology*, Gaithersburg, MD, USA, 2021, DOI: 10.18434/T4D303.

14 P. Masclet, D. Grosjean, G. Mouvier and J. Dubois, *J. Electron. Spectrosc. Relat. Phenom.*, 1973, **2**, 225.

15 K. D. Jordan and P. D. Burrow, *Acc. Chem. Res.*, 1978, **11**, 341–348.

16 M. Jonsson, *J. Phys. Chem.*, 1996, **100**, 6814–6818.

17 P. J. Roden, M. S. Stark and D. J. Waddington, *Int. J. Chem. Kinet.*, 1999, **31**, 277–282.

18 L. Vereecken and B. Nozière, *Atmos. Chem. Phys.*, 2020, **20**, 7429–7458.

19 F. Paulot, J. D. Crounse, H. G. Kjaergaard, A. Kürten, J. M. St Clair, J. H. Seinfeld and P. O. Wennberg, *Science*, 2009, **325**, 730–733.